

PROBING THE INTERGALACTIC MEDIUM WITH THE O VI FOREST

TAOTAO FANG AND GREG L. BRYAN^a^aHUBBLE FELLOW

Department of Physics and Center for Space Research

Massachusetts Institute of Technology

NE80-6081, 77 Massachusetts Avenue, Cambridge, MA 02139

Draft version October 27, 2018

ABSTRACT

Recent STIS and FUSE observations have detected O VI absorption lines at low redshift that are not clearly associated with any galactic system. In this paper, we argue that these lines are due to metal enriched hot gas in the intergalactic medium. Using numerical simulations of a cosmological-constant dominated cosmology, combined with reasonable assumptions about the metallicity distribution, we show that the number density and internal characteristics of these lines are correctly predicted. We find that the O VI is primarily produced by collisional ionization from gas at a few times 10^5 K for lines with equivalent widths larger than 40 mÅ, while weaker lines can also be produced by photo-ionization. The absorption occurs in diffuse gas in filaments at moderate overdensity ($\delta \sim 5 - 100$).

Subject headings: intergalactic medium — quasars: absorption lines — large-scale structure of universe — methods: numerical

1. INTRODUCTION

The census of baryons in the local universe (Fukugita, Hogan & Peebles 1998) indicates that a substantial fraction of the baryonic density predicted by primordial nucleosynthesis remains to be detected. Numerical simulations (Cen & Ostriker 1999a; Davé et al. 2001) predict that a large fraction of this is in the form of a moderately warm/hot ($\sim 10^5 < T < 10^7$ K) component (Warm-hot intergalactic medium, or WHIM). The WHIM is hard to detect directly both because of the difficulty in UV observations as well as due to its relatively low intrinsic density. A promising direction is to look for its signature in absorption lines from background quasars (see Hellsten, Gnedin & Miralda-Escudé 1998; Perna & Loeb 1998; Fang et al. 2001).

Recently, a number of groups have reported detecting the Li-like O VI resonance doublet in far-UV QSO spectra at $z < 2$ (Bergeron et al. 1994; Burles & Tytler 1996; Lopez et al. 1999; Churchill & Charlton 1999, rbh01). Savage, Tripp & Lu (1998) also detected an O VI absorber at $z = 0.225$ without any C IV or N V absorption, indicating that it was either collisionally ionized with a temperature $T \sim 5 \times 10^5$ or photo-ionized with a low density. Tripp & Savage (2000) report an O VI absorption system at $z = 0.14$, possibly associated with a galaxy group and Tripp, Savage & Jenkins (2000) describe five O VI absorbers in the range $0.15 < z < 0.27$. Adopting reasonable assumptions, these authors argued that the total number of baryons associated with these absorbers was significant, comparable to the combined mass in stars, cool gas and cluster gas.

In this paper, we explore the connection between these two ideas in more detail. In particular, we posit that the O VI absorption arises, in large part, in collisionally ionized gas that resides in the sheets, filaments and low density clumps that are naturally produced by gravitational

collapse in hierarchical cosmology. The gas is shock-heated to a range of temperatures, while O VI is only significantly produced in a relatively narrow range around 3×10^5 K. This is near the peak of the cooling curve (e.g. Sutherland & Dopita 1993) and so places a constraint on the density if the gas is not to cool in the Hubble timescale. For gas with 10% solar metallicity at 3×10^5 K, the density must be less than $n_H \leq 10^{-5}$ cm⁻³. Assuming an O VI ionization fraction of 0.15, this requires a path length of 100 kpc to generate a column density of $N_{OVI} = 4 \times 10^{13}$ cm⁻², typical of observed values. While this is a relatively large path length, the Hubble expansion if undisturbed would be only ~ 7 km s⁻¹, which is well within the observed line widths. Therefore, we expect that thermal broadening should dominate and $b \sim 20$ km s⁻¹ for most lines. As we will show; however, colder, photoionized gas can also give rise to O VI absorption. For these lines, which tend to have lower column densities, the predicted line width is considerably smaller. Very recently, a preprint by Cen et al. (2001) has appeared which examines this issue using different simulation techniques; where there is overlap, our results agree reasonably well.

This paper is organized as follows. In section 2 we describe the hydrodynamic simulation and how we synthesize the simulated spectra. Section 3 discusses the results and Section 3 summarizes our main conclusions.

2. METHOD

We use numerical simulations to generate predictions for the observed O VI distribution. In particular, we use a grid-based Adaptive Mesh Refinement (AMR) method (Bryan 1996; Norman & Bryan 1999) that provides both good shock capturing as well as relatively high resolution in dense regions. We simulate a cube $20 h^{-1}$ Mpc on a side with gas and dark matter mass resolution of 6×10^7 and $5 \times 10^8 M_\odot$, respectively. The smallest grid cell (i.e. the best resolution) is 9.8 kpc and occurs in the densest

regions. We assume a cosmological model with a matter density $\Omega_0 = 0.3$, baryon density $\Omega_b = 0.04$, Hubble constant $h = 0.67$ (in units of $100 \text{ km s}^{-1}\text{Mpc}^{-1}$) and cosmological constant $\Omega_\Lambda = 0.7$. The initial density field is drawn from an adiabatic CDM power spectrum as approximated by the formula of Eisenstein & Hu (1998).

We include dark matter and gravity but not radiative cooling or energy/metal injection from SN-driven galactic winds. By comparing a set of cosmological hydrodynamic simulations, Davé et al. (2001) concluded that radiative cooling play a minor role in the evolution of WHIM gas at $z \lesssim 3$ due to its low density. However, these processes can play an important role in metal enrichment of the intergalactic medium (IGM). For instance, *FUSE* has detected O VI absorption in the galactic wind from the prototypical dwarf galaxies (see, e.g., Heckman et al. 2001). Since we do not know the distribution of oxygen a priori in this simulation, we adopt a density dependent metallicity model as derived in the simulations of Cen & Ostriker (1999b). While this is reasonable, we plan to revisit this issue in a future paper using a simulation which self-consistently includes both radiative cooling and metal/energy injection.

To analyze the results, we generate artificial spectra as described in Fang, Bryan & Canizares (2001) and Zhang et al. (1997), both for the 1032 \AA O VI line and the 1216 \AA HI Ly α line. To compute the $f(OVI/O)$ and $f(HI/H)$ fractions, we adopt two models to investigate the effect of collisional ionization and photo-ionization mechanisms. In model A, we use collisional ionization only, with ionization fractions from Mazzotta et al. (1998). In model B, we use Cloudy (version 90.04; Ferland et al. 1998) to generate a grid of temperatures ($10^3 < T < 10^7 \text{ K}$) and densities ($10^{-8} < n(\text{cm}^{-3}) < 10^{-2}$). We included a background radiation field as computed by Haardt & Madau (1996) at $z = 0$ due to the observed quasar distribution. We adopt a mean specific intensity at the Lyman limit of $J_\nu = 2 \times 10^{-23} \text{ ergs s}^{-1}\text{Hz}^{-1}\text{sr}^{-1}$. Since the simulation did not include radiative heating/cooling, the unshocked IGM gas has a temperature which is unrealistically low. For these low temperature (and generally low density) regions, we adopt the relation between temperature and density that has been found in simulations of the Ly α forest: $T = T_0(1 + \delta)^{\gamma-1}$ where $T_0 \sim 5,000 \text{ K}$, and $\gamma = 1.4$ (see, e.g., Zhang et al. 1997; Ricotti, Gnedin, & Shull 2000; Davé & Tripp 2001 for observational support). Here overdensity $\delta = \rho_b / \langle \rho_b \rangle - 1$ and $\langle \rho_b \rangle$ is the mean baryon density of the universe. To fit the simulated spectra we adopt the method developed by Zhang et al. (1997), which should work well for these relatively isolated lines.

3. RESULTS

Figure 1 displays the projected baryon overdensity (panel a), O VI column density (panel b, based on model B), temperature ($10^4 - 10^{7.5} \text{ K}$ in panel c; $10^5 - 10^6 \text{ K}$ in panel d). Comparing panel b with panel a, we find that most of the high column density O VI lines come from regions with overdensities of $\delta \sim 5 - 100$. Collisional ionization is dominant in many of these regions, given their temperatures in the range $10^5 - 10^6 \text{ K}$ (panel d), but some systems are clearly photo-ionized, particularly at the low density end. Note that big clusters and groups are too hot to produce O VI.

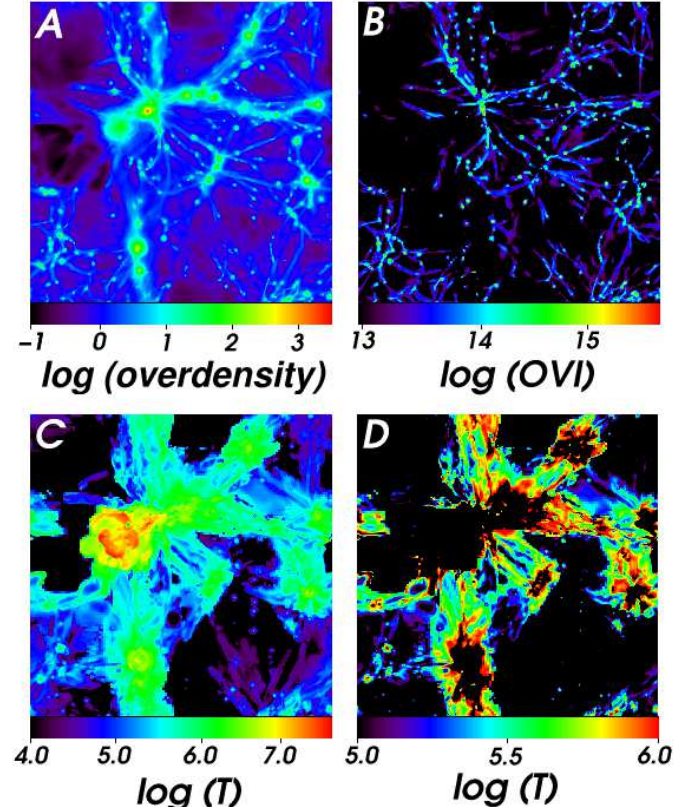


FIG. 1.— Here we show various quantities from the simulation projected along a $5 h^{-1}\text{Mpc}$ line-of-sight; the images are $20 h^{-1}\text{Mpc}$ on a side. Panel a shows the mean baryon overdensity, O VI column density (panel b, in units of cm^{-2}), temperature ($10^4 - 10^{7.5} \text{ K}$ in panel c; $10^5 - 10^6 \text{ K}$ in panel d). Most high column density O VI comes from regions with overdensities of $\delta \sim 5 - 100$ (panel a) and temperatures between $10^5 - 10^6 \text{ K}$ (panel d).

In Figure 2 we show the properties of the simulated region along one random line-of-sight (LOS). From top to bottom we display the baryon number density, peculiar velocity, temperature, O VI number density and transmission spectrum ($F = \exp(-\tau)$, where τ is the optical depth) for O VI in model A (solid line), model B (dashed line) and for H I (dot-dashed line). Model B has been shifted by 5% for visual clarity. Note that at high densities and warm temperatures, both models agree well, while for low temperature regions, model B (which includes both photo- and collisional-ionization), produces substantially more O VI.

Figure 2e shows that both models generate a strong O VI absorption line at around $z \sim 0.0019$ along this LOS. Notice that no strong peak appears in the n and n_{OVI} distributions at the corresponding redshift. This absorption line is actually produced by the n_{OVI} peak at $z \sim 0.0044$. It is the peculiar velocity which shifts the line to a lower redshift: a peculiar velocity of $\sim 750 \text{ km s}^{-1}$ corresponds to a shift of $\Delta z \sim 0.0025$. Parenthetically, we note that this means the total number of lines may be underestimated because the peculiar velocities can shift lines out of the simulated regions; however, we estimate that this would only change our predicted number density by about 10%. Fitting the observed line in Figure 2e gives an equivalent width (EW) of $\sim 185 \text{ m\AA}$ and a Doppler b -parameter of $\sim 21 \text{ km s}^{-1}$, which is roughly consistent with thermal broadening ($b = 0.129(T/A)^{1/2} \text{ km s}^{-1}$, A is the atomic mass number).

Tripp & Savage (2000) suggested that a broad, hot H I Ly α component may coexist with the O VI absorbers and such a broad component could be easy to miss with current observations. To demonstrate this, they showed that a fit to the multicomponent Ly α profile including a broad component (due to H I coexisting with the O VI in hot gas) is indistinguishable from a fit which does not contain such a broad component, at the signal-to-noise level of their data. In Figure 2e we display the H I Ly α spectrum (the dot-dashed line) from our simulation. A broad component is clearly identified at the position of the strongest O VI absorption line. Spectral fitting shows this line has a column density of $3.2 \times 10^{13} \text{ cm}^{-2}$ and a Doppler b -parameter of $\sim 76 \text{ km s}^{-1}$. Both parameters are consistent with those from the missing H I Ly α absorption line in Tripp & Savage (2000). The Doppler b -parameter is also consistent with thermal broadening by a hot gas of $\sim 3 - 4 \times 10^5 \text{ K}$.¹

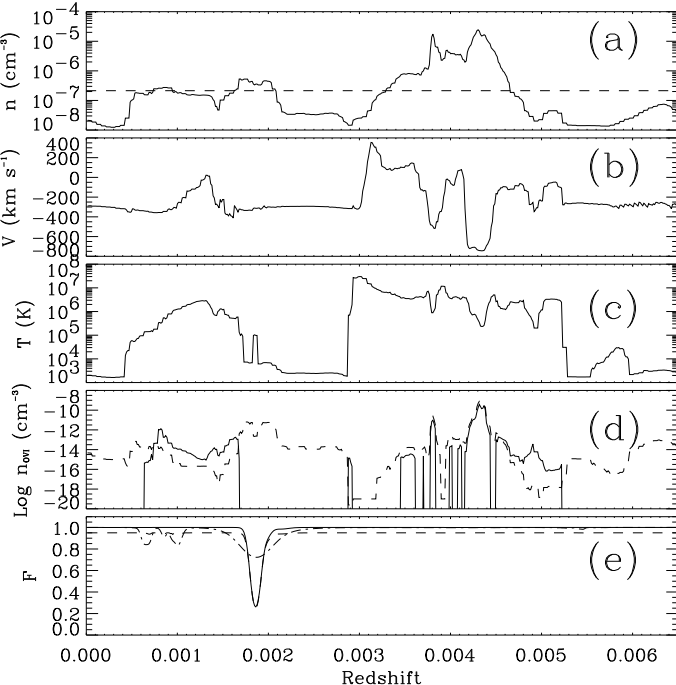


FIG. 2.— Physical properties along one random LOS. (a) baryon number density; (b) peculiar velocity; (c) temperature; (d) O VI number density (model A: solid line; model B: dashed line); (e) synthesized spectra for O VI and H I (dot-dashed line). In panel (d) and (e) model B is shifted down by 5% for visual clarity. The dashed line in panel (a) indicates the mean baryon density. The lines at $z \sim 0.0019$ are produced by gas at $z \sim 0.0044$.

By applying the spectral fit procedure to a total of 3,000 LOS we obtain the cumulative number per unit redshift (dN/dz) as a function of O VI equivalent width. Figure 3 displays the dN/dz for both models. We also plot two observational results from Tripp & Savage (2000) for PG 0953+415 and Tripp, Savage & Jenkins (2000) for E 1821+643. In general we find that the simulation and observations agree reasonably well. We notice that for $EW > 40 \text{ m}\text{\AA}$, the O VI absorption line number per unit redshift from model B is less than twice the line number from model A. This implies that above $EW = 40 \text{ m}\text{\AA}$ the lines from collisionally ionized gas begin to outnumber lines from photo-ionized gas. At $EW > 80 \text{ m}\text{\AA}$, both mod-

els give consistent distributions. This means that those strong lines come from high density and high temperature regions, where collisional ionization dominates. For $EW < 40 \text{ m}\text{\AA}$, lines from photo-ionized gas outnumber lines from collisionally ionized gas, implying that lines produced by photo-ionized gas contribute significantly for low strength lines. Due to our simulation resolution lines with $EW < 20 \text{ m}\text{\AA}$ could be underestimated. Following Rao & Turnshek (2000) and Tripp & Savage (2000) we estimate that at $EW > 40 \text{ m}\text{\AA}$ where collisional ionization dominates, the gas probed by O VI absorption lines is about 10% of the total baryonic matter. This means that the O VI absorption lines can actually probe about $\sim 30\%$ of the WHIM gas, since the fraction of the baryons predicted to be in the WHIM gas is about one third of the total baryonic matter (Davé et al. 2001). The remaining $\sim 70\%$ WHIM gas is likely to be too hot to be detected via O VI absorption: Davé et al. (2001) predicted that at $z = 0$ the baryon fraction peaks at around $4 \times 10^6 \text{ K}$, in which O VII or O VIII should be dominated.

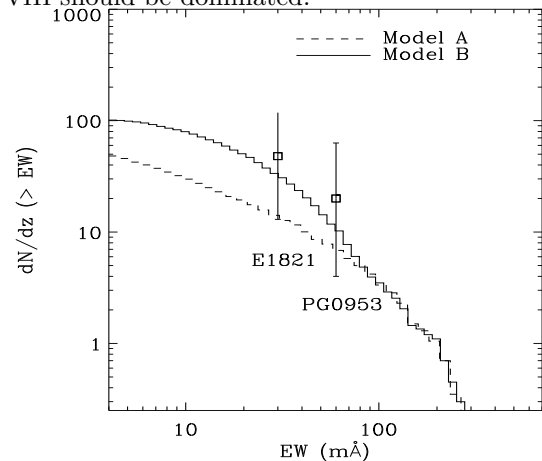


FIG. 3.— Cumulative number of O VI absorption lines per unit redshift vs. line equivalent width. Dashed line: model A; solid line: model B. Lines produced by collisionally ionized gas dominate at $EW > 40 \text{ m}\text{\AA}$. Observational data are plotted with 1σ error bars (Tripp & Savage 2000; Tripp, Savage & Jenkins 2000).

Our result is consistent with what Cen et al. (2001) find in their simulations, especially in that they find at $EW > 35 \text{ m}\text{\AA}$ lines from collisionally ionized gas outnumber lines from photo-ionized gas. However, overall we predict more O VI absorption lines.

We find the Doppler b parameter of the O VI absorption line can provide important clues in distinguishing photo- and collisional-ionization. By fitting the spectra, the Doppler b parameters are obtained for all the O VI absorption lines. We find that the distribution of the line widths is well approximated by a log-normal: $f \propto \exp[-\log^2(b/b_{ln})/2\sigma_{ln}^2]$. In figure 4, we plot b_{ln} against equivalent width cutoff for our two models. In the collisional ionization case (model A), the distribution is nearly constant with $b_{ln} \sim 20 \text{ km/s}$. On the other hand, when we include a photo-ionizing background (model B), the distribution depends on the strength of the line. For lines with $EW > 70 \text{ m}\text{\AA}$, the value of b_{ln} is still around 20 km/s, but drops quickly for smaller lines. This reflects the fact that more photo-ionized lines contribute for

¹A recent observation of the low redshift quasar E 1821+643 (Tripp et al. 2001) reveals that in addition to a narrow H I Ly α line, a relatively broad component appears with $b \approx 85 \text{ km s}^{-1}$ in the $z = 0.1212$ O VI absorption systems.

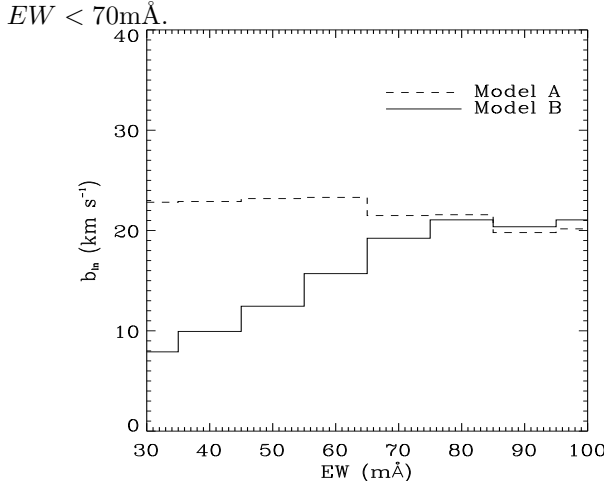


FIG. 4.— The peak of the Doppler b distribution (b_{ln}) for lines with a EW larger than the corresponding value. The value of b_{ln} is obtained by fitting each distribution with a lognormal functional form (solid line: model A; dashed line: model B). The O VI absorption lines that are produced by collisionally ionized gas have a mean b value of ~ 20 km s^{-1} . After including photo-ionized gas, the characteristic b value drops as low as ~ 5 km s^{-1} .

A statistically complete sample does not yet exist to compare against these predictions. Recently Tripp (2001) compiled the first batch of ~ 15 O VI absorption lines detected in a total of five quasars. They found that the majority of the O VI lines have b -values of ~ 22 km s^{-1} , implying a collisional-ionization origin. If this result continues to hold for low equivalent width lines, it may be telling us something either about the strength of the photoionizing background or the metallicity of the low-temperature filaments. Either case (lower background or lower metallicity in the cold gas), would produce fewer photo-ionized lines relative to collisionally ionized.

4. CONCLUSIONS

In this *Letter* we have studied the properties of O VI absorption lines via hydrodynamic simulation. Our main

conclusions are as follows.

1. The projected O VI number density distribution shows that the majority of O VI absorption comes from filaments that connect virialized intersections or groups of galaxies. These regions typically have an overdensity of $\sim 5 - 100$.
2. Spectral fits show that collisional ionization dominates in high density, high temperature regions, while photo-ionization dominates in low density, low temperature regions.
3. The predicted cumulative distribution of O VI absorption lines fits the observations remarkably well, given the uncertainties due to limited resolution and the assumed metallicity distribution. At $EW > 40$ mÅ O VI absorption lines produced by collisionally ionized gas start to outnumber lines produced by photo-ionized gas, while at $EW > 80$ mÅ essentially all the O VI absorption lines are produced by collisionally ionized gas.
4. We find that the O VI absorption lines produced by collisionally ionized gas have a characteristic Doppler b parameter of $\sim 20 - 23$ km s^{-1} , and lines due to the photo-ionized gas typically have narrower b -parameters.

TF thanks the MIT/CXC team for support. This work is supported in part by contracts NAS 8-38249 and SAO SV1-61010. Support for GLB was provided by NASA through Hubble Fellowship grant HF-01104.01-98A from the Space Telescope Science Institute, which is operated by the Association of Universities for Research in Astronomy, Inc., under NASA contract NAS 6-26555.

REFERENCES

Bergeron, J. et al. 1994, ApJ, 436, 33
 Bryan, G. 1996, Ph.D. Thesis
 Burles, S. & Tytler, D. 1996, ApJ, 460, 584
 Cen, R. & Ostriker, J.P. 1999a, ApJ, 514, 1
 Cen, R. & Ostriker, J. P. 1999b, ApJ, 519, L109
 Cen, R., Tripp, T.M., Ostriker, J.P. & Jenkins, E.B. 2001, astro-ph/0106204
 Churchill, C.W. & Charlton, J.C. 1999, AJ, 118, 59
 Davé, R. et al. 2001, ApJ, 552, 473
 Davé, R. & Tripp, T.M. 2001, ApJ, 553, 528
 Eisenstein, D.J. & Hu, W. 1998, ApJ, 498, 137
 Fang, T., Marshall, H.L., Bryan, G.L. & Canizares, C.R. 2001, ApJ, in press
 Fang, T., Bryan, G.L. & Canizares, C.R. 2001, ApJ, submitted
 Ferland, G.J., Korista, K.T., Verner, D.A., Ferguson, J.W., Kingdon, J.B., Verner, E.M. 1998, PASP, 110, 761
 Fukugita, M., Hogan, C.J. & Peebles, J.P.E. 1998, ApJ, 503, 518
 Haardt, F. & Madau, P. 1996, ApJ, 461, 20
 Heckman, T. M., Sembach, K. R., Meurer, G. R., Strickland, D. K., Martin, C. L., Calzetti, D., & Leitherer, C. 2001, ApJ, 554, 1021
 Hellsten, U., Gnedin, N.Y. & Miralda-Escudé, J. 1998, ApJ, 509, 56
 Lopez, S., Reimers, D., Rauch, M., Sargent, W. L. W., & Smette, A. 1999, ApJ, 513, 598
 Mazzotta, P., Mazzitelli, G., Colafrancesco, S. & Vittorio, N. 1998, A&AS, 133, 403
 Norman, M. L. & Bryan, G. L. 1999, ASSL Vol. 240: Numerical Astrophysics, 19
 Perna, P. & Loeb, A. 1998, ApJ, 503, L135
 Rao, S. M. & Turnshek, D. A. 2000, ApJS, 130, 1
 Reimers, D., Baade, R., Hagen, H.-J., & Lopez, S. 2001, A&A, 374, 871
 Ricotti, M., Gnedin, N. Y., & Shull, J. M. 2000, ApJ, 534, 41
 Savage, B.D., Tripp, T.M. & Lu, L. 1998, AJ, 115, 436
 Sutherland, R.S. & Dopita, M.A. 1993, ApJS, 88, 253
 Tripp, T.M. & Savage, B.D. 2000, ApJ, 542, 42
 Tripp, T.M., Savage, B.D. & Jenkins, E.B. 2000, ApJ, 534, L1
 Tripp, T.M., Giroux, M.L., Stocke, J.T., Tumlinson, J. & Oegerle, W.R. 2001, in preparation
 Tripp, T.M. 2001, in preparation
 Zhang, Y., Anninos, P., Norman, M.L. & Meiksin, A. 1997, ApJ, 485, 496